ISSN 0023-1584, Kinetics and Catalysis, 2019, Vol. 60, No. 5, pp. 627–634. © Pleiades Publishing, Ltd., 2019.
Russian Text © The Author(s), 2019, published in Kinetika i Kataliz, 2019, Vol. 60, No. 5, pp. 634–640.

Theoretical Study of the Mechanism of Propionic Acid Deoxygenation on the Palladium Surface

R. S. Shamsiev[a], *, I. E. Sokolov[a], F. O. Danilov[a], and V. R. Flid[a]

[a] *MIREA–Russian Technological University (Lomonosov Institute of Fine Chemical Technologies), Moscow, 119571 Russia*

**e-mail: Shamsiev.R@gmail.com*

Received January 11, 2019; revised April 12, 2019; accepted May 6, 2019

Abstract—Using the DFT–PBE method in the scalar relativistic approximation, the mechanisms of the two main pathways of propionic acid deoxygenation on the rough and flat (111) palladium surfaces have been studied. According to the calculations, in the decarboxylation mechanism on rough and flat surfaces, the formation of the following intermediates is preferable: C_2H_5COO, C_2H_4COO, and C_2H_4. For the second deoxygenation pathway via decarbonylation reactions, the mechanisms on different surfaces of palladium differ. Thus, on a rough surface, the most likely steps are $C_2H_5COOH \rightarrow C_2H_5CO \rightarrow C_2H_5 \rightarrow C_2H_4$, and on the Pd(111) surface the most likely steps are $C_2H_5COOH \rightarrow C_2H_4COOH \rightarrow C_2H_4CO \rightarrow C_2H_4$. The coordination unsaturation of palladium atoms contributes to a decrease in the activation barriers of the reaction by 8–13 kcal/mol. Thus, the flat surface of palladium particles is less active in the deoxygenation of carboxylic acids. The type of palladium surface insignificantly affects the selectivity of deoxygenation. On a rough surface, the decarbonylation rate is slightly higher than the rate of decarboxylation. On the Pd(111) surface, the rate of decarboxylation is higher. The difference in the activation barriers of these pathways of deoxygenation is small (0.7 kcal/mol).

Keywords: carboxylic acid deoxygenation, palladium clusters, Pd(111) surface, decarbonylation, decarboxylation, DFT method

DOI: 10.1134/S0023158419050094

INTRODUCTION

Continued interest in renewable fuels is associated with environmental and economic issues. Over the past 15–20 years, various methods for producing biofuels have been developed (see reviews [1, 2]), based on the cracking of biomass. Together with many other drawbacks of biodiesel produced by such methods, the low heat of combustion is noted due to its high oxygen content in comparison with petroleum fuels. In connection with this, hydrodeoxygenation and deoxygenation processes are of particular interest [3], in which oxygen is removed in the form of CO (decarbonylation), CO_2 (decarboxylation), and H_2O (decarbonylation, hydrodeoxygenation) with the formation of hydrocarbons. The resulting fuel, called "green" or "renewable" diesel, is superior to biodiesel in terms of calorific value and environmental friendliness. Compared with hydrodeoxygenation, deoxygenation of fatty acid triglycerides through decarboxylation and decarbonylation reactions allows the use of simpler catalysts and requires less hydrogen. One of the most active and frequently used fatty acids in deoxygenation are various supported palladium catalysts [4–6].

Recently, some progress has been made in understanding the mechanism of deoxygenation, without which it is difficult to imagine the development of highly efficient catalysts. Earlier, density functional theory (DFT) was used to study the mechanisms of decarboxylation and decarbonylation reactions of propionic acid (as a model of fatty acids) on nonplanar surfaces of Pd_4 [7] and Pd_{15} [2, 8] clusters, and it was shown that C–C bond breaking requires the preliminary abstraction of a hydrogen atom from the β-C atom in a propionic acid molecule. Assuming that in decarboxylation and decarbonylation reactions a common intermediate (Int) is formed with an adsorbed COOH species, the decarbonylation reaction is preferred. The breaking of C–COOH bond has the highest activation barrier ($\Delta^{\neq}G_{623} = 32.8$ kcal/mol).

According to the microkinetic analysis of the deoxygenation of propionic acid on the Pd(111) and Pd(211) surfaces [9] based on periodic DFT-PW91 calculations, the step of dissociation of OC–OH bond (in decarbonylation reaction) and C–COO bond (in decarboxylation reactions) precedes the deep dehydrogenation of the propionic acid molecule to CHCHCOOH or CH_3CCOO species, respectively. In

Table 1. Adsorption energy (kcal/mol) of propionic acid on palladium surfaces

Surface	AC1		AC2		AC3	
	$\Delta_{ads}E_0$	$\Delta_{ads}G_{623}$	$\Delta_{ads}E_0$	$\Delta_{ads}G_{623}$	$\Delta_{ads}E_0$	$\Delta_{ads}G_{623}$
Pd_{13} (a)	−25.8	−0.6	−18.4	7.3	−19.8	10.8
Pd(111) (b)	−14.7	8.5	−6.7	16.8	−3.0	20.3

our opinion, this is a rather controversial idea of the mechanism, which may take place only in the case of the sufficiently strong adsorption of a propionic acid molecule. Moreover, despite ignoring the entropy factor, negligibly small values of the turnover frequency (TOF, ~10^{-7} s^{-1}) were obtained in the work.

The goal of this work was to modeling of the mechanisms of propionic acid decarboxylation and decarbonylation reactions on various models of the palladium surface and to estimate their relative catalytic activity.

METHODS

Quantum chemical calculations were performed using PRIRODA software [10, 11] in the framework of the all-electron scalar relativistic approximation of density functional theory. We used the PBE exchange-correlation functional [12] and an L11 basis set [13] with the following contraction scheme: Pd (26*s*23*p*16*d*5*f*)/[7*s*6*p*4*d*1*f*], C, O (10*s*7*p*3*d*)/[4*s*3*p*1*d*], and H (6*s*2*p*)/[2*s*1*p*]. The applicability of this method was checked for palladium hydride systems [14].

The Pd_{13} icosahedral cluster (rough surface model) and the Pd_{30} two-layer cluster were used as models of the palladium surface. All surface atoms of the Pd_{13} cluster are equivalent and have a lower coordination number (CN = 6), compared to the atoms of the Pd(111) surface (CN = 9). The ground electronic state of the Pd_{13} and Pd_{30} clusters has a spin multiplicity of 9 and 17, respectively. The choice of these models is due to the fact that their structure is almost undeformed upon the adsorption of unsaturated molecules (for example, phenylacetylene [15]), which allows us to exclude the cluster distortion energy from consideration in the calculations.

The correspondence of the optimized structures to minima or transition states (PS) was confirmed by frequency analysis. The coordinates of the palladium atoms were not fixed in the calculations.

The turnover frequency for each route was calculated using the *energetic span* model [16] in the AUTOF program [17]. The Gibbs energy of intermediates (Int) and transition states were calculated for a temperature of 623.15 K corresponding to most of experimental studies of deoxygenation of fatty acids, and the relative sums of the energies were determined for the C_2H_5COOH molecule and a palladium cluster. The resulting change in the Gibbs energy in propionic acid decarboxylation ($\Delta_r G_{623}$ = −37.5 kcal/mol) and decarbonylation ($\Delta_r G_{623}$ = −28.8 kcal/mol) was calculated using the most accurate method CCSD/L11, since there is no need to calculate palladium species for such an estimate.

RESULTS AND DISCUSSION

The modeling of the interaction of the propionic acid molecule with the Pd_{13} cluster and the Pd(111) surface showed that in both cases only three adsorption complexes (AC) can be formed. The optimized structures of the detected adsorption complexes are shown in Fig. 1, and their energies are listed in Table 1.

As follows from Table 1, the strongest complexes are obtained due to the interaction of O and H atoms of the carboxyl group with Pd atoms with the perpendicular arrangement of the acid molecule (AC1a and AC1b, Fig. 1). At the same time, only on the nodes of the Pd_{13} cluster, the $\Delta_{ads}G_{623}$ value is negative (−0.6 kcal/mol for AC1a, Table 1). In other cases, especially for the flat surface (AC1b–AC3b, Table 1), the adsorption energies $\Delta_{ads}E_0$ do not compensate for the loss of entropy during the formation of the adsorption complex. Therefore, with such values of $\Delta_{ads}G_{623}$, it is difficult to imagine and model the mechanisms initiated by the stages of the H atom abstraction from the α- and β-C atoms of the propionic acid molecule [9].

Mechanisms of Decarboxylation and Decarbonylation on Pd_{13}

Since in real conditions of deoxygenation, there is always hydrogen in the system, and in order to limit the migration of adsorbates, preliminary dissociative adsorption of the H_2 molecule on the Pd_{13} surface was modeled. In the presence of H atoms, the adsorption energy of the propionic molecule acid on Pd_{13} slightly increases (by 0.3 kcal/mol).

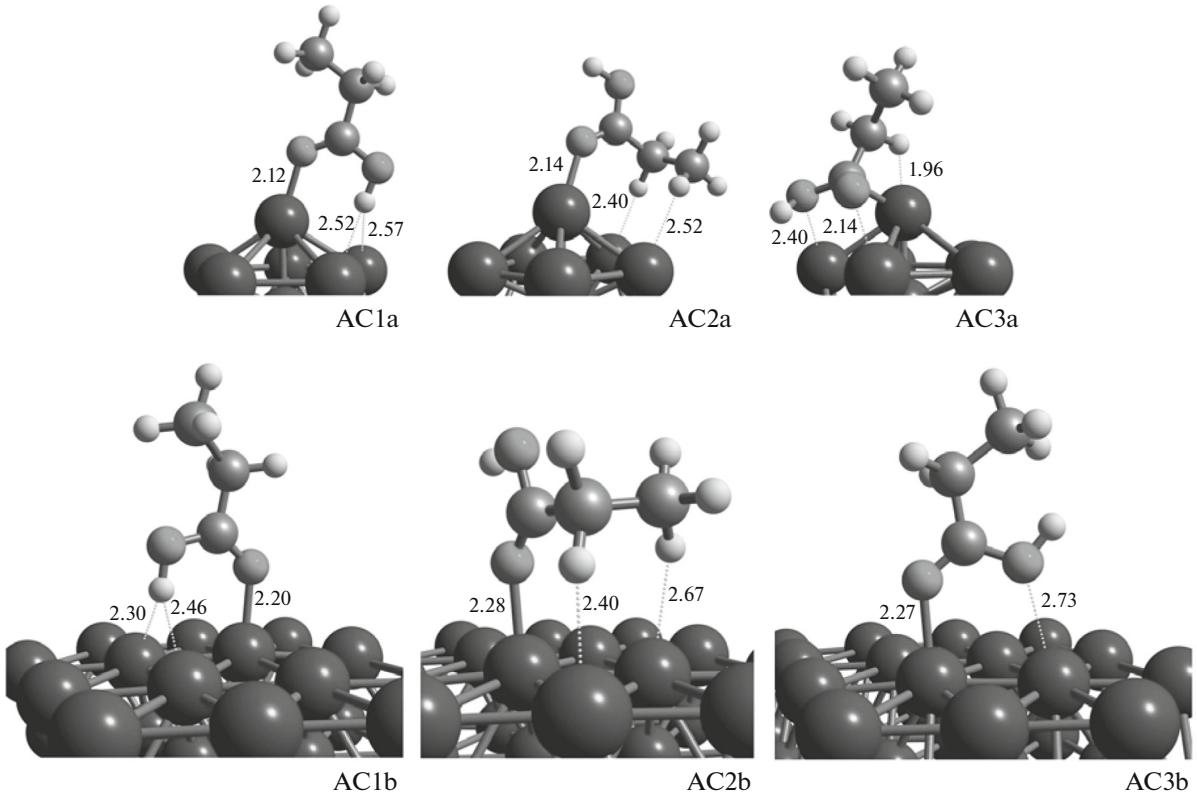

Fig. 1. Structures of adsorption complexes (AC) of propionic acid with the Pd_{13} cluster and Pd(111) surface. Interatomic distances are given in angstroms.

Figure 2 shows the scheme of the transformation of propionic acid in decarboxylation reactions. In the first stage, with a low activation barrier (8.8 kcal/mol), the H atom is abstracted and the $C_2H_5COO^*$ species (Int1a, Fig. 2) is formed on the Pd_{13} surface with μ_2 coordination on Pd atoms leading to a noticeable decrease in energy.

The step of C–C bond breaking in intermediate Int1a has a high activation barrier (35.9 kcal/mol for Int1a → Int2a, Fig. 2). A significantly smaller barrier of C–C bond breaking is required if the H atom is previously abstracted from the β-C atom of $C_2H_5COO^*$ species (Int1a → Int3a, Fig. 2). The abstraction of the H atom from the β-C atom is likely to allow the $C_2H_4COO^*$ species to bind more tightly to the metal and thereby activate the C–C bond. In this case, the cleavage of the carbon–carbon bond in the $C_2H_4COO^*$ species (Int3a) is associated with overcoming a low barrier of 13.5 kcal/mol and the noticeable exothermic effect (Int4a) due to the π-coordination of ethylene. Then, the elimination of the CO_2 molecule almost without an activation barrier is possible, which leads to an additional decrease in the energy of the system to –23.6 kcal/mol (Int5a, Fig. 2). The subsequent stages of the transformation of intermediate Int5a are associated with the consecutive hydrogenation of the adsorbed ethylene molecule to ethane (Int5a → Int6a → Int7a, Fig. 2).

Figure 3 shows the most probable mechanism for the decarbonylation of the C_2H_5COOH molecule. The first step of this mechanism is associated with a change in the coordination of the carboxyl group on palladium (Int1b). From the energy standpoint, this step is unfavorable, since the energy of the system increases to 14.2 kcal/mol, but it creates structural prerequisites for the subsequent steps of C–C bond breaking (Int1b → Int2b, Fig. 3) or abstraction of an OH group (Int1b → Int3b, Fig. 3). From the kinetic point of view, the C–C bond breaking in Int2b (24.1 kcal/mol) is less probable than the C–OH bond breaking (21.5 kcal/mol). In the latter case, the $C_2H_5CO^*$ species is formed with a small decrease in energy (Int3b, Fig. 3).

The abstraction of the hydrogen atom from the β-C atom of $C_2H_5CO^*$ species occurs with a higher activation barrier (20.6 kcal/mol for Int3b → Int4b, Fig. 3) compared to the barrier of the C–C bond cleavage (9.6 kcal/mol for Int3b → Int5b). Moreover, the step Int3b → Int5b is accompanied by a noticeable decrease in the energy of the system in contrast to the

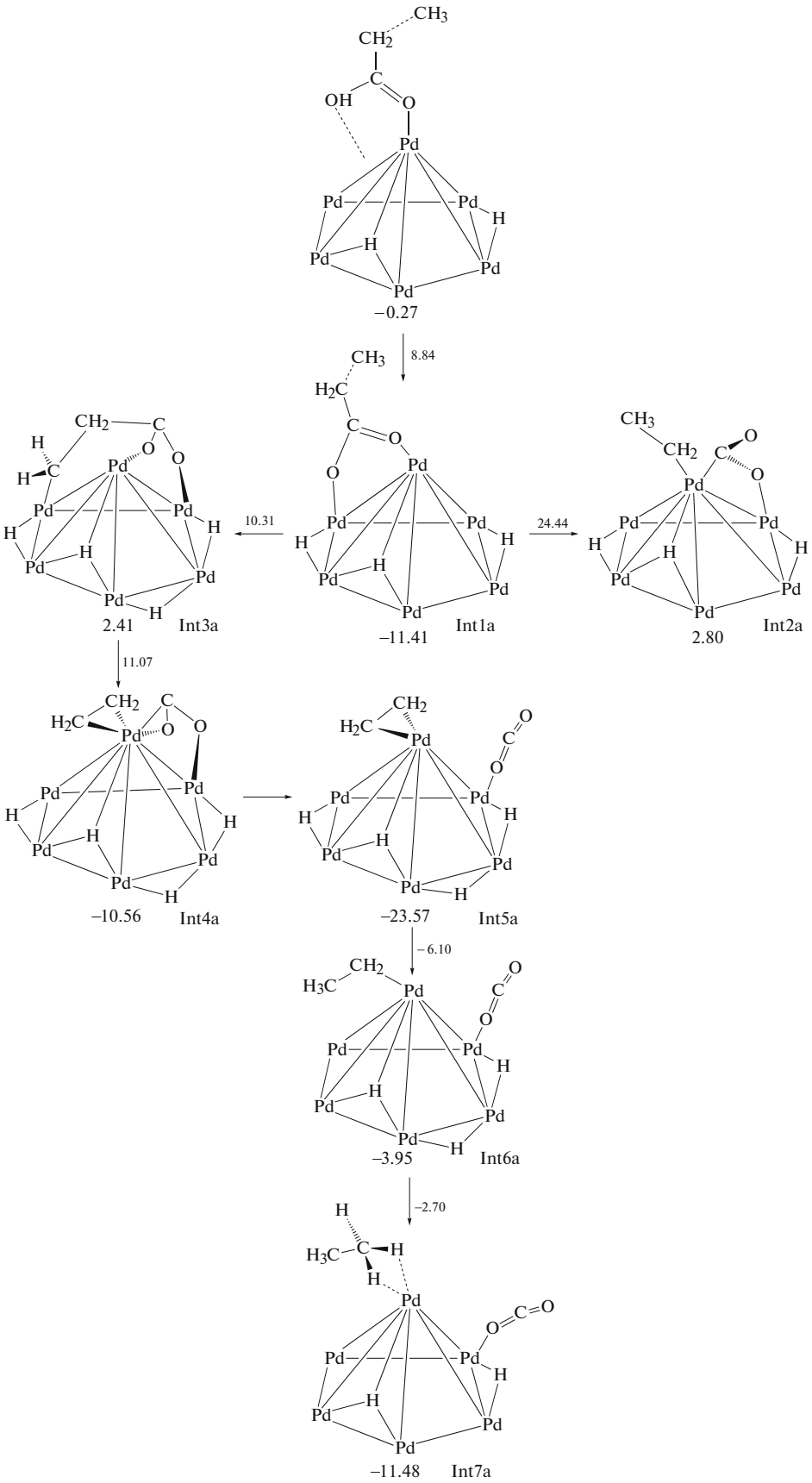

Fig. 2. Mechanism of decarboxylation of propionic acid on Pd_{13}. The values of ΔG_{623} are given next to the description of structures, the values of $\Delta^{\neq} G_{623}$ (in kcal/mol) are shown near the arrows.

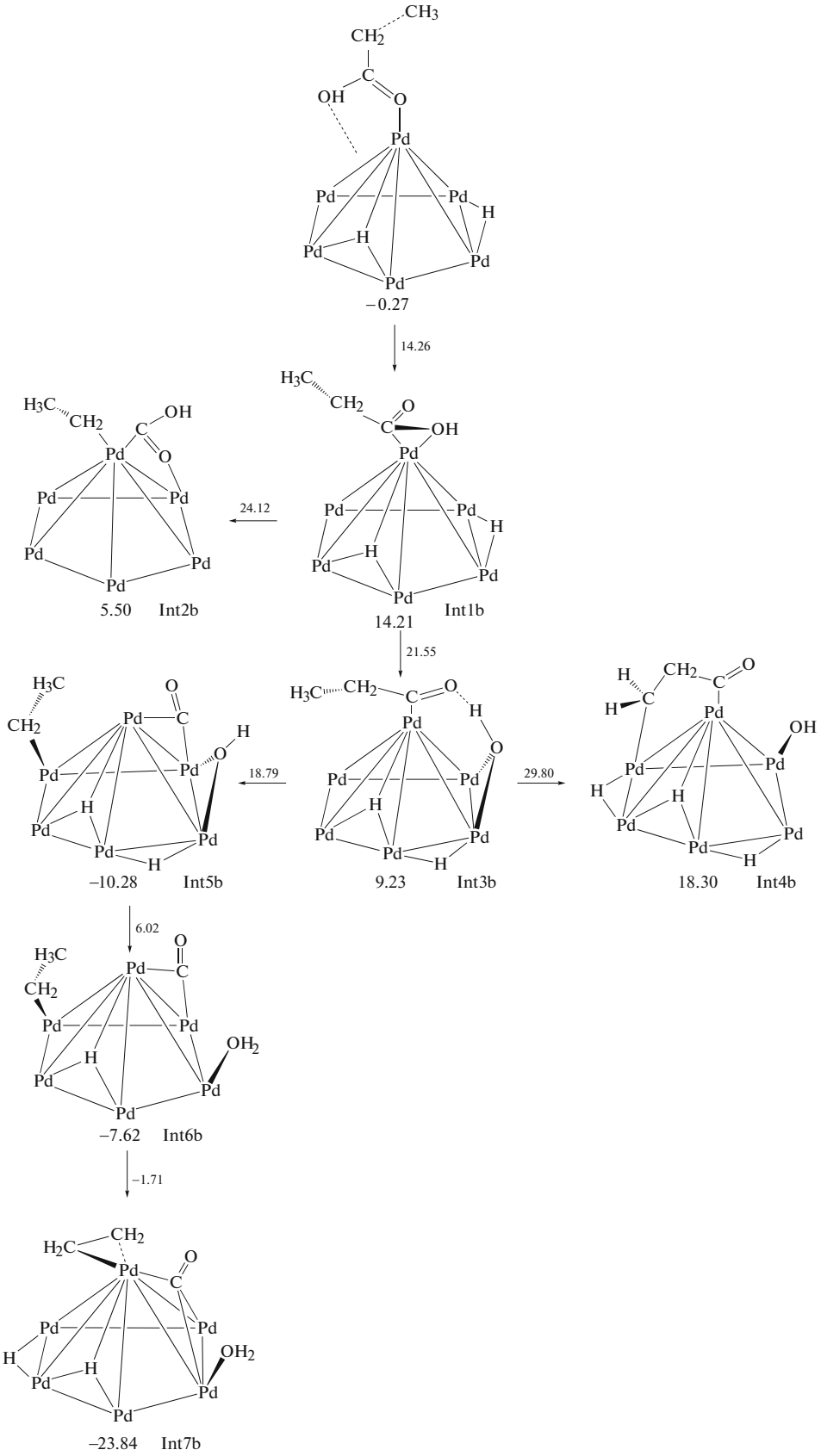

Fig. 3. Mechanism of decarbonylation of propionic acid on Pd_{13}. The values of ΔG_{623} are given next to the description of structures, the values of $\Delta^{\neq} G_{623}$ (in kcal/mol) are shown near the arrows.

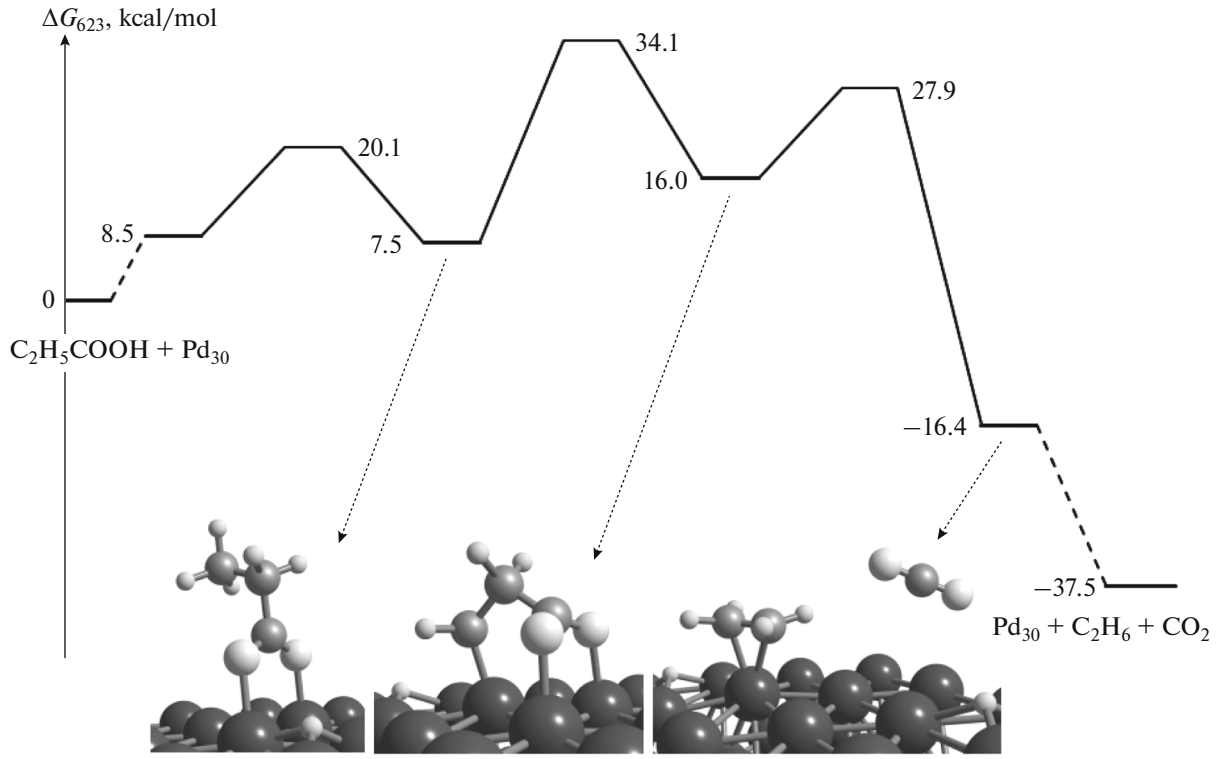

Fig. 4. Energy profile of decarboxylation of propionic acid on the Pd(111) surface.

step Int3b → Int4b. The final steps of the formation of a water molecule (Int5b → Int6b, Fig. 3) and dehydrogenation of ethyl to ethylene (Int6b → Int7b, Fig. 3) do not require overcoming significant activation barriers. Thus, the maximum energy barriers of decarboxylation and decarbonylation reactions on the Pd_{13} surface are 22.5 and 21.8 kcal/mol, respectively.

Mechanisms of Decarboxylation and Decarbonylation Reactions on the Pd(111) Surface

Figures 4 and 5 show the energy profiles and optimized structures of intermediates of the decarboxylation and decarbonylation reactions on the Pd(111) surface. As calculations showed, the mechanism of decarboxylation reaction on a flat surface (Fig. 4) generally corresponds to the decarboxylation mechanism on a rough surface (Fig. 2). The main difference lies in a sharp increase in the activation barriers of each step (by 8–12 kcal/mol) starting with the adsorption of the propionic acid molecule. Apparently, the main reason for these changes is the low coordination accessibility of atoms on the flat surface of palladium.

As for the decarbonylation reaction mechanism, we failed to detect the intermediate Int1b with the activated C–OH bond on a flat surface (Fig. 3). In this regard, the C–OH bond breaking should be preceded by the step of hydrogen atom abstraction from the β-C atom of the propionic acid molecule with the formation of C_2H_4COOH species (Fig. 5). Otherwise, the TS energy of the step of C–OH bond breaking in the C_2H_5COOH molecule reaches a value of 38.4 kcal/mol (Fig. 5).

Figures 4 and 5 show that the overall activation barriers of decarboxylation and decarbonylation reactions are quite close (34.1 and 34.8 kcal/mol), and the corresponding calculated TOF values (14.1 and 4.2 s^{-1}) are 7–8 orders of magnitude higher than the similar values given in [9].

CONCLUSIONS

Quantum chemical modeling (DFT-PBE/L11 method) of propionic acid deoxygenation on the palladium surface revealed the most probable (low-energy) mechanisms of the main directions of the process—decarboxylation and decarbonylation. The decarboxylation mechanism includes the steps of adsorption of propionic acid, the consecutive abstraction of hydrogen atoms from the carboxyl group and β-carbon atom, the cleavage of the C–C bond with the elimination of the CO_2 molecule and, finally, the hydrogenation of ethylene to ethane. The β-elimination of the hydrogen atom (in the case of Pd(111)) and the C–C bond breaking (in the case of Pd_{13}) have the highest activation barriers.

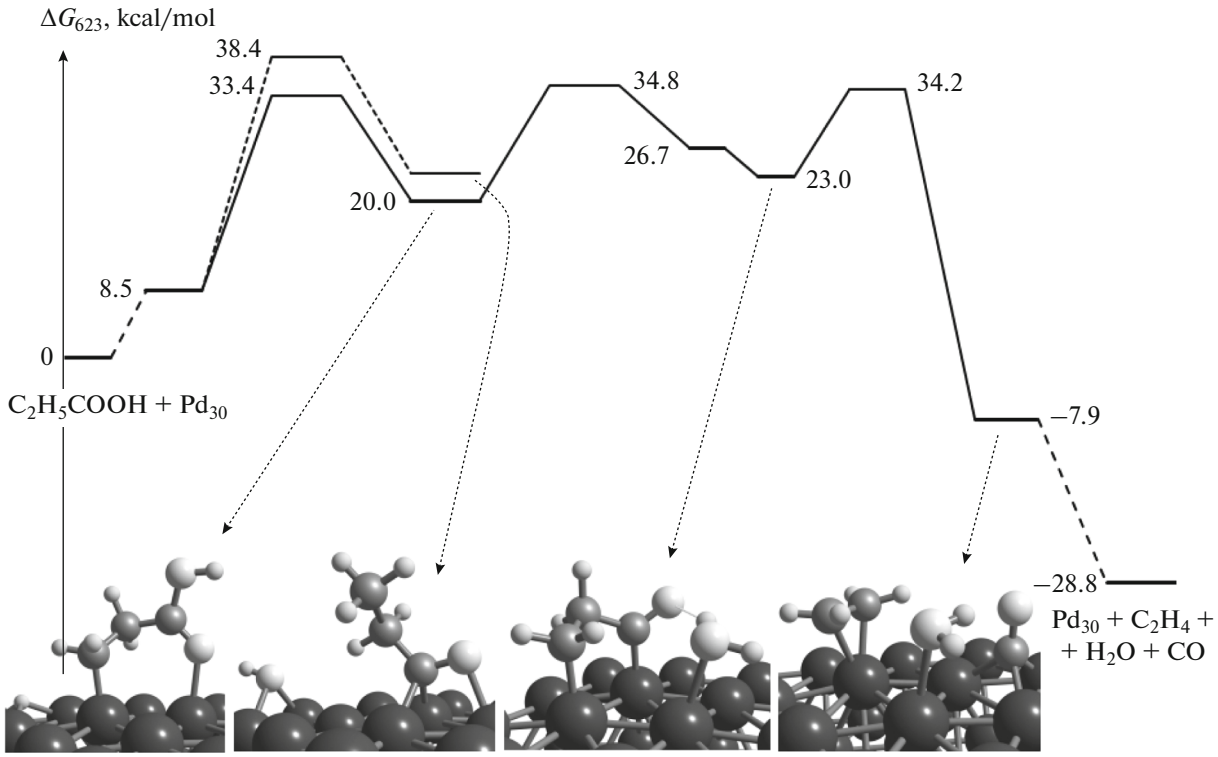

Fig. 5. Energy profiles of decarbonylation of propionic acid on the Pd(111) surface.

The mechanism of decarbonylation reaction on the rough surface includes the following sequence of intermediates: $C_2H_5COOH \rightarrow C_2H_5CO \rightarrow C_2H_5 \rightarrow C_2H_4$. On the Pd(111) surface, the sequence of intermediates is somewhat different: $C_2H_5COOH \rightarrow CH_2CH_2COOH \rightarrow C_2H_4CO \rightarrow C_2H_4$. The abstraction of the OH group has the maximal activation barrier.

According to calculations, the coordination accessibility of the surface palladium atoms of the Pd_{13} cluster contributes to a decrease in the activation barriers by 8–13 kcal/mol. Thus, the type of palladium surface structure has a significant effect on the rate of the process, and the flat surfaces of palladium species are less active in the deoxygenation of carboxylic acids. At the same time, the TOF values of the decarboxylation and decarbonylation reactions on Pd(111) are quite high: 14.1 and 4.2 s^{-1}, respectively.

Despite the different nature of the limiting steps of the deoxygenation directions, their activation barriers are very close within the same surface type, which explains the experimentally observed set of products characteristic of both directions. For a rough surface the decarbonylation reaction rate is slightly higher than the decarboxylation rate. For the Pd(111) surface, the opposite is true. In both cases, the difference in the activation barriers of these directions of deoxygenation is small (0.7 kcal/mol) and is within the limits of error of density functional theory.

ABBREVIATIONS AND NOTATION

AC	adsorption complex
CN	coordination number
DFT	density functional theory
Int	intermediate
TOF	turnover frequency

FUNDING

This work was supported by grant no. 18-03-00689 from the Russian Foundation for Basic Research. The calculations were carried out using the computing resources of the Joint Supercomputer Center of the Russian Academy of Sciences and Moscow State University.

REFERENCES

1. Santillan-Jimenez, E. and Crocker, M., *J. Chem. Technol. Biotechnol.*, 2012, vol. 87, p. 1041.
2. Berenblyum, A.S., Danyushevsky, V.Ya., Kuznetsov, P.S., Katsman, E.A., and Shamsiev, R.S., *Pet. Chem.*, 2016, vol. 56, no. 8, p. 663.
3. Berenblyum, A.S., Podoplelova, T.A., Shamsiev, R.S., Katsman, E.A., Danyushevsky, V.Ya., and Flid, V.R., *Catalysis in Industry*, 2012, vol. 4, no. 3, p. 209.

4. Snåre, M., Kubicková, I., Mäki-Arvela, P., Eränen, K., and Murzin, D.Yu., *Ind. Eng. Chem. Res.*, 2006, vol. 45, p. 5708.
5. Berenblyum, A.S., Podoplelova, T.A., Shamsiev, R.S., Katsman, E.A., and Danyushevsky, V.Ya., *Pet. Chem.*, 2011, vol. 51, no. 5, p. 336.
6. Ford, J.P., Immer, J.G., and Lamb, H.H., *Top. Catal.*, 2012, vol. 55, p. 175.
7. Berenblyum, A.S., Shamsiev, R.S., Podoplelova, T.A., and Danyushevsky, V.Ya., *Russ. J. Phys. Chem. A*, 2012, vol. 86, no. 8, p. 1199.
8. Berenblyum, A.S., Podoplelova, T.A., Katsman, E.A., Shamsiev, R.S., and Danyushevsky, V.Ya., *Kinet. Catal.*, 2012, vol. 53, no. 5, p. 595.
9. Behtash, S., Lu, J., Williams, C.T., Monnier, J.R., and Heyden, A., *J. Phys. Chem. C*, 2015, vol. 119, no. 4, p. 1928.
10. Laikov, D.N., *Chem. Phys. Lett.* 1997, vol. 281, p. 151.
11. Laikov, D.N. and Ustynyuk, Yu.A., *Russ. Chem. Bull.*, 2005, no. 3, p. 820.
12. Perdew, J.P., Burke, K., and Ernzerhof, M., *Phys. Rev. Lett.*, 1996, vol. 77, p. 3865.
13. Laikov, D.N., *Chem. Phys. Lett.*, 2005, vol. 416, p. 116.
14. Shamsiev, R.S. and Danilov, F.O., *Russ. Chem. Bull.*, 2017, vol. 66, no. 3, p. 395.
15. Shamsiev, R.S. and Danilov, F.O., *Kinet. Catal.*, 2018, vol. 59, no. 3, p. 333.
16. Uhe, A., Kozuch, S., and Shaik, S., *J. Comput. Chem.*, 2011, vol. 32, p. 978.
17. Kozuch, S. and Martin, J.M.L., *ACS Catal.*, 2011, vol. 1, p. 246.

Translated by Andrey Zeigarnik